JHU-2545 Selectively Shields Salivary Glands and Kidneys during PSMA-Targeted Radiotherapy

Michael T. Nedelcovych[1,2], Ranjeet P. Dash[1,2], Ying Wu[1], Eun Yong Choi[8], Rena S. Lapidus[8], Pavel Majer[9], Diane Abou[11], Marie-France Penet[4,7], Anastasia Nikolopoulou[10], Alex Amor-Coarasa[10], John Babich[10], Daniel L. Thorek[11], Rana Rais[1,2], Clemens Kratochwil[12], Barbara S. Slusher[1,2,3,4,5,6*]

[1]Johns Hopkins Drug Discovery, Departments of [2]Neurology, [3]Medicine, [4]Oncology, [5]Psychiatry, [6]Neuroscience, [7]Radiology and Radiological Science, Johns Hopkins School of Medicine, Baltimore, MD 21205, U.S.A.

[8]Translational Laboratory Shared Service, University of Maryland School of Medicine, 655 West Baltimore Street, Baltimore, MD, 21201, U.S.A.

[9]Institute of Organic Chemistry and Biochemistry, Academy of Sciences of the Czech Republic v.v.i., Prague, 166 10, Czech Republic

[10]Division of Radiopharmaceutical Sciences and MI(3), Department of Radiology, Weill Cornell Medicine, New York, NY, U.S.A.

[11]Depatment of Radiology, Washington University School of Medicine, Saint Louis, MO, 63110, U.S.A.

[12]Department of Nuclear Medicine, University Hospital Heidelberg, Heidelberg, Germany

Address Correspondence to:

*Barbara S. Slusher, PhD, Johns Hopkins Drug Discovery, 855 North Wolfe Street, Baltimore, Maryland, USA 21205, Phone: 410-614-0662, Fax: 410-614-0659, E-mail: bslusher@jhmi.edu

Keywords: PSMA, radiopharmaceutical, prodrug, mCRPC, dosimetry

STATEMENT OF TRANSLATIONAL RELEVANCE

Prostate Specific Membrane Antigen (PSMA) molecular radiotherapy has emerged as a promising treatment for metastatic castration-resistant prostate cancer (mCRPC), but endogenous expression of PSMA in kidneys and salivary glands causes uptake into these organs resulting in dose-limiting toxicities. We describe the discovery of JHU-2545, a PSMA inhibitor prodrug that selectively blocks kidney and salivary gland uptake of PSMA theranostics without altering tumor uptake in both preclinical models and in mCRPC patients. Pretreatment of JHU-2545 thereby improves the safety and efficacy profile of the multiple PSMA radiotherapies in development.

ABSTRACT

PURPOSE: Prostate-specific membrane antigen (PSMA) radiotherapy is a promising treatment for metastatic castration-resistant prostate cancer (mCRPC) with several beta or alpha particle-emitting radionuclide-conjugated small molecules showing efficacy in late stage patients. However, PSMA is also expressed in kidneys and salivary glands where specific uptake causes dose-limiting xerostomia and potential for nephrotoxicity. The PSMA inhibitor 2-(phosphonomethyl)pentanedioic acid (2-PMPA) can prevent kidney uptake in mice, but also blocks tumor uptake, precluding its clinical utility. Selective delivery of 2-PMPA to non-malignant tissues could improve the therapeutic window of PSMA radiotherapy.

EXPERIMENTAL DESIGN: A tri-alkoxycarbonyloxy alkyl (TrisPOC) prodrug of 2-PMPA, JHU-2545, was synthesized to enhance 2-PMPA delivery to non-malignant tissues. Preclinical pharmacokinetic and imaging experiments were conducted prior to assessment in 3 mCRPC patients receiving PSMA PET and radiotherapy.

RESULTS: JHU-2545 resulted in 3- and 53-fold greater exposure of 2-PMPA in rodent salivary glands (18.0 ± 0.97 h*nmol/g) and kidneys (359 ± 4.16 h*nmol/g) versus prostate tumor xenograft (6.79 ± 0.19 h*nmol/g). JHU-2545 also blocked rodent kidneys and salivary glands uptake of the PSMA PET tracers ^{68}Ga-PSMA-11 and ^{18}F-DCFPyL by up to 85% without effect on tumor. In a mCRPC patient, JHU-2545 treatment prior to ^{68}Ga-PSMA-617 administration reduced kidney SUV_{max} by 76% without effect on metastatic lesions. When administered prior to injection of the beta emitter ^{177}Lu-PSMA-617, JHU-2545 shielded both the salivary glands (72% Gy reduction) and kidneys (45% Gy reduction) without effect on metastases' dose.

CONCLUSIONS: JHU-2545 pre-treatment raises the cumulative dose limit and improves the safety and efficacy profile of PSMA radiotherapy.

INTRODUCTION

PSMA molecular radiotherapy has emerged as a promising treatment for mCRPC (1-3). PSMA is highly upregulated (10-100 fold) in the majority of prostate cancer lesions (4,5), and though its functional role in malignancy is unclear, the degree to which PSMA surface expression is increased correlates with disease progression, androgen independence, and metastasis (4,5). Furthermore, ligand binding to PSMA induces rapid internalization, enriching the agent inside the cell and promoting accumulation within PSMA-expressing tissues (4,5).

These observations have led to the development of a family of small molecule PSMA ligands conjugated to positron or beta or alpha particle-emitting radionuclides suitable for mCRPC PET imaging (e.g. ^{18}F-DCFPyL, ^{68}Ga-PMSA-11, ^{68}Ga-PSMA-617), beta therapy (e.g. ^{177}Lu-PSMA-617, ^{131}I-MIP-1095), or alpha therapy (e.g. ^{225}Ac-PSMA-617) (6,7). Some of these molecules, such as PSMA-617, contain a chelator functional group that enables labeling with isotopes for use as both imaging and therapeutic agents (7,8). For example, ^{177}Lu-PSMA-617 has been administered to hundreds of late stage mCRPC patients after confirming PMSA radioligand uptake into metastases with ^{68}Ga-PSMA-617 or similar PSMA PET tracers (8-10). These reports, including results from a Phase 2 trial of ^{177}Lu-PSMA-617 (ACTRN12615000912583) (11), indicate promising efficacy in heavily pre-treated patients who have exhausted benefit from approved therapies (9,10). Dozens of randomized clinical trials are now registered to confirm the utility and efficacy of PSMA imaging and radiotherapy, with ^{177}Lu-PSMA-617 having recently entered Phase 3 trials in mCRPC (NCT03511664).

Despite significant progress, clinical development of PSMA-targeted agents has been complicated by the physiologic expression of PSMA in normal tissues including salivary glands and kidneys (12,13) which exhibit avid uptake of PSMA radiopharmaceuticals during imaging

and radiation dosimetry (5,8). Salivary gland uptake of PSMA radiotherapeutics can result in transient or permanent xerostomia, an adverse effect particularly problematic for alpha radionuclides (2,14). For example, ^{225}Ac-PSMA-617 recently showed striking efficacy in heavily pre-treated mCRPC patients (5/40 complete tumor control >2 years), but this impressive response was nearly matched by treatment discontinuation due to xerostomia (4/40) (2). For beta emitters such as ^{177}Lu-PSMA-617, kidney accumulation represents the cumulative dose-limiting toxicity, leading to risk of nephrotoxicity that restricts the number of allowable cycles (4,5,10,15-20). Repeated cycles have been associated with improved efficacy and response rate, suggesting that this limitation could result in sub-optimal outcomes (10,21-23). Importantly, due to increased risk of delayed/chronic renal disease, this restriction also precludes the use of PSMA radiotherapeutics earlier in disease course despite initial indications of superior efficacy relative to approved third-line treatments (3,11,24). Randomized controlled trials of PSMA radiotherapeutics as first or second-line treatments are expected in the near future with trial designs incorporating cumulative kidney exposure as a potential activity-dose/cycle limit.

In an attempt to mitigate healthy tissue exposure during PSMA radiotherapy, the highly selective PSMA inhibitor (2-PMPA; IC_{50}=0.3nM) has been evaluated for its ability to block radioligand uptake in the salivary glands and kidneys through direct competitive displacement at a shared PSMA binding site (16,19). In one study, 2-PMPA (0.01 mg) co-injection with ^{177}Lu-PSMA I&T (100 MBq) reduced the absorbed dose to the kidneys by 83% and attenuated nephrotoxicity 3 months later in mice bearing PSMA-expressing human cancer xenografts (19). Although encouraging, these results did not prompt clinical testing because 2-PMPA also inhibited tumor uptake of the radiotherapeutic by more than 50%, resulting in accelerated tumor growth and significantly reduced overall survival relative to mice that received the radiotherapeutic alone (19).

Similar results were obtained when 2-PMPA was paired with ^{125}I-MIP-1095 (16). Thus, although 2-PMPA provided an important proof-of-concept for the shielding approach, co-treatment with this molecule could not strike a balance between salivary gland/kidney displacement versus tumor uptake that could improve the therapeutic index of PSMA radiotherapy.

Herein we describe the discovery of a tri-alkoxycarbonyloxy alkyl (TrisPOC) 2-PMPA prodrug termed JHU-2545, which was found to preferentially deliver 2-PMPA to non-malignant tissues such as salivary glands and kidneys versus prostate adenocarcinoma. In rodent pharmacokinetic studies, JHU-2545 exhibited a 3- and 53-fold enhanced delivery of 2-PMPA to salivary glands and kidneys, respectively, versus prostate cancer xenografts. In further support of this finding, pre-treatment with JHU-2545 was shown to block ^{68}Ga-PSMA-11 uptake in rat kidneys and ^{18}F-DCFPyL uptake in mouse salivary glands and kidneys by up to 85% without effect on prostate cancer xenograft uptake. Based on these encouraging pharmacokinetic and imaging data in preclinical studies, JHU-2545 (10 mg, i.v.) was subsequently administered to mCRPC patients under compassionate care. In a within-subject comparison, JHU-2545 pre-treatment prior to ^{68}Ga-PSMA-617 administration reduced kidney tracer uptake by 76% of SUV_{max} while only causing a 3% mean reduction of SUV_{max} in metastases. In mCRPC patients receiving ^{177}Lu-PSMA-617, JHU-2545 shielded both the salivary glands (72% dose reduction in Gy) and kidneys (45% dose reduction in Gy) without any significant effect on radiotherapeutic dose in the metastases. JHU-2545 pre-treatment may thus raise the cumulative dose limit and improve the safety and efficacy of PSMA radiotherapy.

MATERIALS AND METHODS

Animals. All animal experiments were conducted in compliance with NIH guidelines and with the approval of the Institutional Animal Care and Use Committees at Johns Hopkins University, the University of Maryland, and Weill Cornell Medicine and were undertaken in accordance with the guidelines set forth by the USPHS Policy on Humane Care and Use of Laboratory Animals. All rodents were maintained on a 12 hour light-dark cycle with unrestricted access to food and water. Adult male NSG mice were obtained from UMB Vet Resources and used for *in vivo* pharmacokinetic studies. Adult male Sprague-Dawley rats (500-550g) were obtained from Taconic and used for ^{68}Ga-PSMA-11 PET imaging studies. Adult male 8 wk FVB and Nu/Nu mice were used for ^{18}F-DCFPyL PET studies. Nu/Nu mice were implanted with 5x10^{6} 22RV1 cells in a 1:1 PBS:matrigel mixture and allowed to grow to approximately 250 mm^{3} (3 weeks).

Compounds. 2-PMPA was obtained from Sigma Aldrich (St. Louis, MO). JHU-2545 was synthesized and characterized as previously described by our group (Compound 21b) (25). Clinical-grade ^{18}F-DCFPyL was formulated under good manufacturing practices as previously described (26,27) at the Johns Hopkins University School of Medicine PET Center (at specific activities of approximately 3 Ci/µmol). The precursor PSMA-617 (10 mM in DMSO) was obtained as GMP-grade from ABX Advanced Biochemical Compounds (Radeberg, Germany). For preparation of ^{68}Ga-PSMA-617, solutions of 2 µL PSMA-617, 300 µl Natriumacetate (2.5 M in water) and 10 µL ascorbic acid (20% in water) were added to 1 mL of $^{68}Ga^{3+}$ eluate from a ^{68}Ge/^{68}Ga radionuclide generator (iThemba Labs). The pH of the labeling solution was adjusted to 3,5 – 4 and the mixture was incubated at 95 °C for 10 minutes. The product was purified by solid-phase extraction (Sep-Pak Light tC18, Waters), washing was performed with a 0.9% NaCl solution and for elution ethanol was used. Purity was confirmed by reversed-phase HPLC. ^{177}Lu-PSMA-

617 for patient use was prepared as previously described (9). Briefly, PSMA-617 was dissolved in dimethyl sulfoxide to obtain a 10 mM solution. Two microliters (20 nmol) of this solution were used per 1 GBq of ^{177}Lu-LuCl3 (EndolucinBeta, Isotope Technologies, Garching, Germany, 0.04 M HCl) mixed with 10 µL of 20% ascorbic acid and 100 µL of 0.4 M sodium acetate buffer (pH 5; adjusted with acetic acid) and injected directly into the ^{177}Lu-LuCl3 delivery vial. After being heated to 95°C for 10 minutes, a quality check per reversed-phase high-performance liquid chromatography and instant thin-layer chromatography was performed, and the final product was diluted in 2 mL of 0.9% NaCl.

Mouse Pharmacokinetics. To generate a C4-2 *in vivo* model, 3x10^6 LNCaP-C4-2 cells (kind gift of Miriam Smith PhD, University of Maryland School of Medicine) were subcutaneously injected into the flanks of male NSG mice (UMB Vet Resources). When tumors grew to approximately 600-800 mm^3, tumors were excised, aseptically cut into 2mm x 2mm pieces and frozen back viably (5% DMS0/95% FBS). Tumors were not passaged from mouse to mouse more than 4 times. For the current experiment, two vials of viably frozen explants were thawed at 37 °C. Tumor explants were washed in RPMI without FCS and then surgically implanted in a subcutaneous pocket in male NSG mice. When tumors reached 600-800 mm^3, mice were euthanized, tumors excised aseptically, and cut into 2mm x 2mm pieces prior to re-implantation into 40 mice. When tumors reached 500-700 mm^3, the pharmacokinetic experiment was performed. 2-PMPA (3 mg/kg, i.v.) or a molar equivalent of JHU-2545 (7.62 mg/kg, i.v.) were injected via tail vein after dissolution in vehicle (5% EtOH/10% Tween 80/ 85% 50mM HEPES). Mice were then euthanized under isoflurane anesthesia 0.25, 0.5, 1, 3, or 6 hours post-dose (n=3/group). Blood was collected by cardiac puncture into EDTA-lined tubes and stored on ice until plasma was isolated by

centrifugation. Salivary glands, kidneys, and tumor were harvested and flash frozen on dry ice. All tissues were stored at -80 °C prior to bioanalysis.

Rodent PET Imaging. PET acquisitions for rat ^{68}Ga-PSMA-11 were performed with a Biograph mCT scanner (Siemens Healthcare, Malvern, PA, USA) in groups of 4 animals. Rats were anesthetized with isoflurane (Henry Schein Animal Health, Melville, NY) at 2-2.5% in oxygen for induction, and 1.5-2% in oxygen for maintenance. After induction of anesthesia, an i.v. catheter was inserted into the tail vein of each rat. The animals were then positioned in the camera in transaxial position with its body in the center of the field of view. Thirty minutes before radiotracer administration, rats were treated with either vehicle or JHU-2545 at 1 or 10 mg/kg of body weight via the i.v. catheter (0.5 mL/rat, n= 2/group). JHU-2545 stock solution was prepared in 10% EtOH in PBS. ^{68}Ga-PSMA-11 (42±5 MBq/rat) was injected as a bolus (~0.5 mL) and a 60-min dynamic scan started with 12 × 5min time frames. For all the acquisitions, a CT scan of 8.9 sec was performed before PET scan, for attenuation correction. The list-mode data were iteratively reconstructed with TrueX+TOF (UltraHD PET) (2 iterations, 21 subsets) after being normalized and corrected for attenuation, scatter and decay with final images having a voxel size of 2.06 mm (2.0×1.02×1.02). Volumes of Interest (VOIs) were manually drawn onto the dynamic PET images to extract time-activity curves and %ID/g values. All image analyses were performed using the AMIDE software. Mice undergoing ^{18}F-DCFPyL PET imaging were administered radiotracer (7.4-9 MBq) either anesthetized (isoflurane) on camera with a tail vein catheter for kinetic studies, or via the retroorbital sinus for static images. A dedicated high resolution small animal PET scanner (R4, Concorde Microsystems; 7.8 cm axial by 10 cm transaxial field of view) was used to acquire whole body mouse scans (in the prone position) in list-mode configuration with a 350-700 keV energy range and a coincidence-timing window of 6 nsec for a minimum of 20x10^6 coincident

events as previously described (28). PET image data were corrected for detector non-uniformity, dead time, random coincidences and physical decay and normalized to injected activity (determined by Capintec CR15 dose calibrator with setting #457). All images were reconstructed using the 3D maximum a posteriori (3D-MAP) algorithm. Acquisition Sinogram and Image PROcessing software (Siemens) were used to place three-dimensional regions of interest volumes of interest at the regions of the tumors, salivary glands, heart and kidneys for analysis. Time-activity curves were generated after administration of vehicle or JHU-2545 (5mg/kg, i.v.) 5-60 minutes prior to ^{18}F-DCFPyL bolus dosing (n=2-3/group). JHU-2545 dose effects were assessed by administration of vehicle or JHU-2545 (0.05-5mg/kg, i.v.) 15 minutes prior to ^{18}F-DCFPyL bolus dosing (n=2-3/group).

Bioanalysis. Bioanalysis to determine 2-PMPA concentrations after protein precipitation was conducted by LC–MS/MS as previously described (25,29). Detailed methods are also provided as supplementary information.

Pharmacokinetic and Statistical Analysis. Non-compartmental-analysis module in Phoenix WinNonlin version 7.0 (Certara USA, Inc., Princeton, NJ) was used to assess pharmacokinetic parameters. Peak plasma concentrations (C_{max}) were the observed values. Area under the curve (AUC) was calculated by log–linear trapezoidal rule to the end of sample collection (AUC_{last}). Comparisons between rat kidney uptake of ^{68}Ga-PSMA-11 were conducted by one-way ANOVA with Dunnett's post hoc test. Comparisons between mouse kidney, salivary gland, and tumor uptake of ^{18}F-DCFPyL were conducted by two-tailed *t*-test. Significance was defined as $P < 0.05$.

Patients. PSMA-617 was offered as surrogate therapy in accordance with the updated Declaration of Helsinki, paragraph-37 "Unproven Interventions in Clinical Practice," and in accordance with German regulations (§13(2b) German Pharmaceutical Act) for "compassionate use," which

includes priority of all approved treatments (without contraindications) and confirmation of the indication by both a nuclear medicine physician and an external expert in urology or oncology. Both patients treated with ^{177}Lu-PSMA-617 were castration resistant to LHRH-analogs plus bicalutamide and secondary hormone manipulation with abiraterone; one patient with 110kg body-weight and age 68y was also resistant against docetaxel, the other with 78kg body-weight and age 76y was considered unfit for chemotherapy. No systematic patient selection was performed, except both patients presented with a PSMA-positive tumor phenotype based on PSMA PET imaging. A third patient (84kg, age 53y) was evaluated with ^{68}Ga-PSMA-617 with and without JHU-2545 pre-treatment, but due to his low tumor burden the experimental therapy was postponed. All patients were informed about the experimental nature of this intervention and gave written informed consent. The ethical committee approved this retrospective observational study. Dosimetry data from historical controls presented herein are derived from patients treated under the same protocol at our center as previously reported (9).

^{68}Ga-PSMA-617 PET. PET/CT imaging was performed on a Biograph mCT Flow scanner (Siemens, Erlangen, Germany). PET was acquired in 3-D mode (matrix 200×200) using FlowMotion (Siemens). The emission data was corrected for randoms, scatter and decay. Reconstruction was performed with an ordered subset expectation maximization (OSEM) algorithm with two iterations/21 subsets and Gauss-filtered to a transaxial resolution of 5 mm at full-width at half-maximum (FWHM). Attenuation correction was performed using an unenhanced low-dose CT that was reconstructed to a slice thickness of 5 mm, increment of 3–4 mm, soft tissue reconstruction kernel (B30), and acquired using CareDose (Siemens) noise equivalent to 30mAs/130keV.

^{177}Lu-PSMA-617 Dosimetry. Dosimetry analyses were performed using QDOSE dosimetry software suite (ABX-CRO advanced pharmaceutical services Forschungsgesellschaft m.b.H), as previously reported (9). Detailed methods are also provided as supplementary information.

RESULTS

JHU-2545 preferentially delivered 2-PMPA to mouse salivary glands and kidneys versus prostate cancer xenograft. Concentrations of 2-PMPA in plasma, tumor, salivary glands, and kidneys were measured at multiple time points after tail vein administration of either 2-PMPA or JHU-2545 (3mg/kg or molar equivalent, i.v.) to NSG mice harboring subcutaneous xenografts of human C4-2 prostate cancer cells. JHU-2545 administration resulted in 2-PMPA plasma, kidney, and salivary gland exposures of 17.8 ± 1.02 h*nmol/mL, 359 ± 4.16 h*nmol/g, and 18.0 ± 0.97 h*nmol/g, respectively (Figure 1). Kidney and salivary gland exposures were 53- and 3-fold greater than those observed in the tumor (6.79 ± 0.19 h*nmol/g) (Figure 1). When directly compared to 2-PMPA administration, kidney:tumor and salivary:tumor 2-PMPA concentration ratios over time were increased several fold by JHU-2545 with no significant effect on the plasma:tumor ratio (Figure S1).

JHU-2545 pre-treatment dose-dependently attenuated uptake of PSMA radioligands in rodent salivary glands and kidneys. Kidney shielding was first confirmed by PET imaging after administration of JHU-2545 (1 or 10 mg/kg, i.v.) to rats 30 minutes prior to ^{68}Ga-PSMA-11 (42±5 MBq) bolus dosing. PET images clearly showed differences in renal uptake and retention with greater cortical uptake and retention in the saline control animals (Figure 2A, top) compared with the animals treated with JHU-2545 (Figure 2A, bottom). In the dynamic PET scans, JHU-2545 treated rats show reduced renal cortical retention of radiotracer compared to controls with rapid flux through the renal pelvis with activity rapidly passing into the bladder. Time activity curves derived from the ROI data (Figure 2B) show a dose effect with a modest drop in activity at 1 mg/kg JHU-2545 and a more dramatic effect at 10 mg/kg JHU-2545. Using the trapezoid method, area

under the curve for each treatment arm was calculated; compared to controls, there was a significant reduction of 20% and 69% in the integrated kidney dose at 1 and 10 mg/kg JHU-2545, respectively [$F(2, 3) = 95.28$; $p = 0.0019$] (Figure 2C).

JHU-2545 at a dose of 0.25mg/kg and a pre-treatment time of 15 minutes optimally shielded rodent kidneys and salivary glands with no effect on prostate cancer tumor uptake. A dose response (0.05 – 5mg/kg, i.v.) and time course (5 – 60 min pre-treatment) of JHU-2545 was subsequently evaluated for kidney and salivary gland blocking in non-tumor bearing mice assessing uptake of ^{18}F-DCFPyL by PET. Administration of JHU-2545 (5mg/kg, i.v.) 15 minutes prior to tracer administration was found to optimally attenuate radioligand uptake in both organs as assessed by time-activity curves (Figure 3A). With this pre-treatment time, JHU-2545 achieved maximal radioligand shielding in the kidneys and salivary glands between 0.2 and 1mg/kg (Figure 3B). Representative PET images at 1 hour post-tracer injection exhibit robust, dose-dependent clearance of ^{18}F-DCFPyL from the renal cortex and salivary glands of mice pre-treated with JHU-2545 (Figure 3C). To ensure minimal interference with tumor uptake, the lowest efficacious dose of JHU-2545 was subsequently used to assess kidney and salivary gland shielding in 22RV1 tumor-bearing mice. When administered 15 minutes prior to injection of ^{18}F-DCFPyL (7.4-9 MBq, i.v.), JHU-2545 (0.25 mg/kg, i.v.) blocked salivary gland and kidney uptake but had no effect on tumor uptake of radioligand at 60 minutes post-tracer injection relative to mice pre-treated with vehicle (Figure 3D). Vehicle vs. JHU-2545 pre-treatment, respectively, resulted in salivary gland uptake of 0.78 ± 0.19 vs. 0.10 ± 0.03 %ID/g [$t(6) = 8.27$; $p = 0.0002$]; kidney uptake of 34.21 ± 5.36 vs. 2.6 ± 0.52 %ID/g [$t(8) = 13.1$; $p < 0.0001$]; and tumor uptake of 4.48 ± 2.23 vs. 4.17 ± 1.49 %ID/g [$t(8) = 0.26$; $p = 0.7988$] (Figure 3D). JHU-2545 pre-treatment thus afforded 85 and 87% mean reductions in kidney and salivary gland uptake of PSMA radioligand at 60 minutes, but

had no effect on tumor uptake, substantially improving the tumor:kidney and tumor:salivary uptake ratios (Figure 3D). Thus, JHU-2545 at a dose of 0.25mg/kg and a pre-treatment time of 15 minutes was found to provide optimal selective shielding.

JHU-2545 pre-treatment attenuated uptake of ^{68}Ga-PSMA-617 in mCRPC patient salivary glands and kidneys but not metastases. Avid uptake of PSMA radioligand in metastases (SUV_{max} 3.6 – 12.5), parotid gland (SUV_{max} 18.2), submandibular gland (SUV_{max} 23.1), and kidneys (SUV_{max} 35.4) was first confirmed in a mCRPC patient by PET scan 1 hour after administration of ^{68}Ga-PSMA-617 (235 MBq, 20 nmol, i.v.) (Figure 4). When administered 15 minutes prior to injection of ^{68}Ga-PSMA-617 in the same patient on a subsequent day (265 MBq, 20nmol, i.v.), JHU-2545 (10 mg, i.v.) reduced radioligand uptake in parotid gland (SUV_{max} 10.6), submandibular gland (SUV_{max} 14.6), and kidneys (SUV_{max} 8.5) but had no significant effect on metastases (SUV_{max} 3.9 – 8.8) (Figure 4). Quantified as a within-subject percent change, JHU-2545 reduced salivary gland and kidney uptake by 37 and 76%, respectively; in contrast, a 3% mean change was observed in metastases (Figure 4).

JHU-2545 pre-treatment attenuated ^{177}Lu-PSMA-617 doses in mCRPC patient salivary glands and kidneys but not metastases. Two mCRPC patients received JHU-2545 (10 mg, i.v.) 15 minutes prior to injection with ^{177}Lu-PSMA-617 (7.4 GBq, 150 nmol, i.v.). Representative images from one of the mCRPC patient is shown (Figure 5). First, PSMA avid lesions as well as significant uptake of ^{68}Ga-PSMA-617 was observed in kidneys and salivary glands during a diagnostic PET scan without JHU-2545 pre-treatment (Figure 5A, left). Time-dependent planar imaging in this patient after administration of ^{177}Lu-PSMA-617 with JHU-2545 pre-treatment

revealed persistent uptake into metastases with reduced exposure in the kidneys and salivary glands (Figure 5A, right). Relative to historical controls from the same center (9), JHU-2545 pre-treatment reduced ^{177}Lu-PSMA-617 mean absorbed dose to the kidneys and salivary glands (Figure 5B), resulting in doses of 0.38 and 0.37 Gy/GBq, respectively, for patient 1, and 0.43 and 0.45 Gy/GBq, respectively, for patient 2 (Table S1). These values fall below the standard deviation of historical controls treated and analyzed at the same center, and represent mean absorbed dose reductions of 48% and 72% for the kidneys and salivary glands, respectively (Figure 5B; Table S1). JHU-2545 also reduced the lacrimal gland dose by 82% (Table S1). In contrast, JHU-2545 pre-treatment had no significant effect on the dose to metastases. Patient 1 exhibited a mean metastases' dose of 8.03 Gy/GBq, and patient 2 exhibited a mean metastases' dose of 13.15 Gy/GBq (Figure 5B; Table S1). Both of these values fall within the standard deviation of historical controls (Figure 5B; Table S1), and are at or above absorbed dose values reported to result in therapeutic efficacy (9). In contrast to other organs, JHU-2545 appeared to cause a slight increase in the red marrow dose (Table S1), a finding consistent with the interpretation that competitive displacement of the radiotherapeutic from other tissues increased its circulation time. However, this red marrow dose was still within the range reported in other dosimetry studies (see below) and is not considered dose-limiting.

Healthy organ dosimetry estimates for the historical control patients used as direct comparators in this study fall very near median values previously reported for other mCRPC patients receiving therapeutic or sub-therapeutic concentrations of ^{177}Lu-PSMA-617 (9,15,21,30-34). Controls in the current report exhibited mean absorbed doses to the salivary glands of 1.44 Gy/GBq (reported range: 0.72-1.90 Gy/GBq), to the kidneys of 0.78 Gy/GBq (reported range:

0.53-0.99 Gy/GBq), and to the red marrow of 0.03 Gy/GBq (reported range: 0.01-0.05 Gy/GBq), and can thus be considered representative.

JHU-2545 pre-treatment increased metastases:organ dose ratios and raised the estimated cumulative allowable dose of ^{177}Lu-PSMA-617. In addition to the historical controls used as direct comparators in this study, JHU-2545 pre-treated patients were compared to patients from two other reports in which both healthy organ and mCRPC metastases dosimetry was conducted for ^{177}Lu-PSMA-617 (30,33). JHU-2545 pre-treatment compared favorably to both control cohorts, increasing the metastases:salivary gland dose ratio to between 350% and 550% of control values, and the metastases:kidney dose ratio to between 190% and 650% of control values (Table 1). Based on estimated radiation-absorbed dose limits of 30 Gy for the salivary glands (15) and 28 Gy for the kidneys (35), the cumulative ^{177}Lu-PSMA-617 dose expected to reach the critical threshold for these organs based on reported mean dosimetry values is between 21 and 36 GBq (Table S2). Based on dosimetry in the patients that received JHU-2545 pre-treatment, this cumulative allowable ^{177}Lu-PSMA-617 dose is increased to between 60 and 74 GBq (Table S2). Thus, based on available dosimetry, JHU-2545 increases the cumulative allowable ^{177}Lu-PSMA-617 dose by 2 to 6-fold.

DISCUSSION

PSMA radiotherapy is a promising treatment for mCRPC with multiple radionuclide-conjugated small molecule PSMA ligands in clinical development (6,7,36). ^{177}Lu-PSMA-617 has shown efficacy in hundreds of mCRPC patients, but high specific uptake into salivary glands and kidneys has resulted in xerostomia and potential for nephrotoxicity (5,8). We show that a novel prodrug, JHU-2545, alters the biodistribution and preferentially delivers the PSMA inhibitor 2-PMPA to the salivary glands and kidneys, shielding these dose-limiting organs from exposure to PSMA radiopharmaceuticals without hindering tumor uptake.

Direct injection of 2-PMPA results in shielding of prostate cancer as well as normal organs, precluding its clinical use. Other efforts to shift specific uptake of PSMA radiopharmaceuticals to malignant tissues have included structural modification of PSMA-targeting moieties (37-39). For example, recent attempts were made to improve tumor exposure by conjugating an albumin-binding moiety to PSMA-617 (37,38) or PSMA I&T (39), as well as other urea-based (37) or phosphoramidate-based scaffolds (40). These analogues exhibited prolonged plasma half-life and delivered larger radiation doses to mCRPC xenografts, but full organ radiation dosimetry in a first clinical test recently revealed concurrent increases in kidney and salivary gland doses that translated to even worse tissue:tumor ratios (38).

Wide-ranging but ultimately unsuccessful attempts have also been made to non-specifically mitigate kidney and salivary gland toxicities. These strategies have included co-administration of gelofusine (19) and mannitol (41) to inhibit renal reabsorption, facial application of ice packs to reduce salivary gland blood flow (42), and salivary gland injection of botulinum toxin (43), all of which offered little or no benefit with the exception of the latter. However, this invasive approach has no effect on kidneys and its benefit needs to be confirmed in larger, more

controlled studies. Thus, to our knowledge, kidney and salivary gland protection mediated by JHU-2545 represents the first example of a clinically viable method for enhancing the therapeutic index of PSMA radiotherapeutics.

Salivary gland protection mediated by JHU-2545 may be of immediate clinical utility given that transient or irreversible xerostomia after PSMA radiotherapy has already been reported in a large number of cases (9,10,14). Results from a Phase 2 trial of ^{177}Lu-PSMA-617 in mCRPC found xerostomia to be a very common adverse event, occurring in 87% of patients (11). Co-treatment with 2-PMPA was previously found to have no beneficial effect for salivary glands (16). This finding is consistent with our preclinical pharmacokinetic data indicating little to no salivary gland penetration of 2-PMPA, likely owing to its high polarity and generally poor tissue penetration (25). By contrast, JHU-2545 delivered micromolar concentrations of 2-PMPA to the salivary glands, resulting in a 10-fold improvement in exposure relative to equimolar 2-PMPA. In addition to the salivary glands, JHU-2545 shielded the lacrimal glands from ^{177}Lu-PSMA-617. One recent report predicted the lacrimal glands to be the first organ to reach a critical threshold after ^{177}Lu-PSMA-617 therapy, receiving a mean effective dose of 2.82 Gy/GBq (31). This value is similar to that reported in another recent study (33) as well as to that obtained in the historical controls presented herein (Table 2). Relative to these mean control values, JHU-2545 pre-treatment resulted in a dose reduction to the lacrimal glands of about 82%, suggesting potential to prevent dry eyes as well as dry mouth.

JHU-2545 also delivered high exposures of 2-PMPA to the kidneys and shielded these radiosensitive organs from radiopharmaceutical exposure. The kidneys are considered a dose-limiting organ for PSMA radiotherapies (9,16) based on an estimated critical radiation dose of 28 Gy (biological effective dose) above which risk of chronic renal disease significantly increases

(35). Reported kidney dose estimates for ^{177}Lu-PSMA-617 range from 0.53 to 0.99 Gy/GBq (9,15,21,30-34) so this threshold is predicted to be passed after cumulative administration of between 28 and 52 GBq. When observed kidney doses in JHU-2545 pre-treated patients are compared to the most conservative kidney doses previously reported, JHU-2545 more than doubles the calculated treatment limit. Critically, this benefit does not appear to come at the expense of metastatic absorbed-dose, with calculated doses well within previously reported ranges (9,30,33) known to be efficacious (9). JHU-2545 may therefore substantially increase the cumulative dose of PSMA radiotherapy that can be administered. Recent reports indicate that repeated dosing of PSMA radiotherapeutics prolongs tumor control (23) such that an appreciable increase in the allowable cumulative dose could improve efficacy.

It is important to note, however, that severe nephrotoxicity has not yet been observed in the mCRPC patients treated with PSMA radiotherapies to date. This may be due to the fact that these treatments have thus far only been offered to late stage, heavily pre-treated mCRPC patients with resistant disease and survival times of only 1-2 years, whereas radiation-induced kidney failure requires about 2 or more years to manifest (44). Thus, although PSMA radiotherapy has exhibited impressive efficacy in this subgroup, poor prognosis has likely masked the emergence of renal disease.

Although ^{177}Lu-PSMA-617 is initially being tested in late stage mCRPC patients (NCT03511664) (11), consistent signs of efficacy suggest that PSMA radiotherapy will likely have clinical benefit earlier in disease course. A recent meta-analysis found that PSMA radiotherapy exhibits a biochemical response rate double that of recently approved third-line treatments including cabazitaxel and enzalutamide (3). Another compassionate use trial found earlier initiation of PSMA radiotherapy to result in improved survival times (24). PSMA radiotherapy

will thus likely offer greater benefit as a first or second line treatment in mCRPC, or in cooperative or synergic combination with approved drugs (24,45). Furthermore, sizable patient subgroups identifiable with biomarkers such as the truncated androgen receptor variant AR-V7 have recently been shown to exhibit resistance to androgen receptor signaling inhibitors including enzalutamide and abiraterone (46), necessitating alternative treatment options. In all these scenarios, survival rates would almost certainly surpass the time at which renal disease manifests, and kidney protection would become paramount. A controlled head-to-head comparison of ^{177}Lu-PSMA-617 versus cabazitaxel is now underway (NCT03392428) and may soon provide more direct evidence supporting earlier initiation of PSMA-targeted radiotherapy in mCRPC.

A shielding strategy may also be necessary to enable the use of PSMA-targeted alpha therapies such as ^{225}Ac-PSMA-617 (47-49). These radionuclides appear to be more effective than their beta counterparts, but also carry greater risk of severe xerostomia and nephrotoxicity even in late stage mCRPC patients (48,49). For example, a recent report of ^{225}Ac-PSMA-617 showed striking efficacy in very late stage mCRPC patients, with 5 of 40 individuals exhibiting complete tumor control for more than 2 years (2). But this unprecedented response was nearly matched by dropout, with 4 of 40 patients discontinuing treatment due to xerostomia (2). Furthermore, these improved survival times increase the risk of observing delayed nephrotoxicity and may preclude the application of subsequent treatment cycles. This problem is exacerbated by the observation that alpha therapies may overcome resistance to beta emitters, and could provide greatest benefit as a follow-on treatment in refractory patients (2,48). This would likely necessitate reducing the cumulative dose to kidneys incurred during both beta and alpha therapy. In addition, PSMA radiotherapy delivers higher doses to healthy organs in patients with lower tumor volumes (50). Thus, patients with low tumor burden or those exhibiting regression after their first treatment

cycle(s) may be at greater risk for kidney and salivary gland toxicity in subsequent cycles. A protection approach such as that offered by JHU-2545 would be important in this context to ensure that sufficient radiotherapeutic doses could be administered to realize the full benefit of the treatment. JHU-2545 pre-treatment or a similar protection approach may thus be necessary to enable the broadest, most effective use of these therapies.

Although confirmation in larger controlled trials is necessary, combination therapy with JHU-2545 could meaningfully mitigate observed toxicities associated with PSMA radiotherapeutics such as xerostomia, and possibly prevent the emergence of nephrotoxicity. JHU-2545 may thus improve the tolerability, safety, and efficacy of PSMA radiotherapy in mCRPC patients.

Acknowledgements

This research was supported by a Maryland TEDCO MII award (to BSS) and the Institute of Organic Chemistry and Biochemistry of the Academy of Sciences of the Czech Republic v.v.i. DA and DLT were supported in part by NIH/NCI R01CA201035. We thank the JHU PET Center for providing [^{18}F]DCFPyL.

Author Contributions

MTN and BSS conceived the concept, contributed to rodent experimental designs, and wrote the manuscript. PM synthesized JHU-2545. MTN, RPD, YW, EYC, RSL, and RR conducted the rodent pharmacokinetic studies and bioanalysis. DA, MFP, AN, AAC, JB, and DLT conducted the rodent imaging studies. CK conducted all patient treatment, imaging, and dosimetry.

Competing Financial Interests

No competing financial interests.

Supplementary Data and Methods

Supporting Information for this article including supplementary Tables and Materials & Methods are available in the online version of the paper.

References

1. Fendler WP, Rahbar K, Herrmann K, Kratochwil C, Eiber M. (177)Lu-PSMA Radioligand Therapy for Prostate Cancer. J Nucl Med 2017;58(8):1196-200.

2. Kratochwil C, Bruchertseifer F, Rathke H, Hohenfellner M, Giesel FL, Haberkorn U, *et al.* Targeted alpha-Therapy of Metastatic Castration-Resistant Prostate Cancer with (225)Ac-PSMA-617: Swimmer-Plot Analysis Suggests Efficacy Regarding Duration of Tumor Control. J Nucl Med 2018;59(5):795-802.

3. von Eyben FE, Roviello G, Kiljunen T, Uprimny C, Virgolini I, Kairemo K, *et al.* Third-line treatment and (177)Lu-PSMA radioligand therapy of metastatic castration-resistant prostate cancer: a systematic review. Eur J Nucl Med Mol Imaging 2017.

4. Bouchelouche K, Turkbey B, Choyke PL. PSMA PET and Radionuclide Therapy in Prostate Cancer. Semin Nucl Med 2016;46(6):522-35.

5. Ristau BT, O'Keefe DS, Bacich DJ. The prostate-specific membrane antigen: lessons and current clinical implications from 20 years of research. Urol Oncol 2014;32(3):272-9.

6. Eiber M, Fendler WP, Rowe SP, Calais J, Hofman MS, Maurer T, *et al.* Prostate-Specific Membrane Antigen Ligands for Imaging and Therapy. J Nucl Med 2017;58(Suppl 2):67s-76s.

7. Virgolini I, Decristoforo C, Haug A, Fanti S, Uprimny C. Current status of theranostics in prostate cancer. Eur J Nucl Med Mol Imaging 2018;45(3):471-95.

8. Afshar-Oromieh A, Babich JW, Kratochwil C, Giesel FL, Eisenhut M, Kopka K, *et al.* The Rise of PSMA Ligands for Diagnosis and Therapy of Prostate Cancer. J Nucl Med 2016;57(Suppl 3):79s-89s.

9. Kratochwil C, Giesel FL, Stefanova M, Benesova M, Bronzel M, Afshar-Oromieh A, *et al.* PSMA-Targeted Radionuclide Therapy of Metastatic Castration-Resistant Prostate Cancer with 177Lu-Labeled PSMA-617. J Nucl Med 2016;57(8):1170-6.

10. Rahbar K, Ahmadzadehfar H, Kratochwil C, Haberkorn U, Schafers M, Essler M, *et al.* German Multicenter Study Investigating 177Lu-PSMA-617 Radioligand Therapy in Advanced Prostate Cancer Patients. J Nucl Med 2017;58(1):85-90.

11. Hofman MS, Violet J, Hicks RJ, Ferdinandus J, Ping Thang S, Akhurst T, *et al.* [(177)Lu]-PSMA-617 radionuclide treatment in patients with metastatic castration-resistant prostate cancer (LuPSMA trial): a single-centre, single-arm, phase 2 study. Lancet Oncol 2018.

12. O'Keefe DS, Bacich DJ, Heston WD. Comparative analysis of prostate-specific membrane antigen (PSMA) versus a prostate-specific membrane antigen-like gene. Prostate 2004;58(2):200-10.

13. Silver DA, Pellicer I, Fair WR, Heston WD, Cordon-Cardo C. Prostate-specific membrane antigen expression in normal and malignant human tissues. Clin Cancer Res 1997;3(1):81-5.

14. Taieb D, Foletti JM, Bardies M, Rocchi P, Hicks R, Haberkorn U. PSMA-Targeted Radionuclide Therapy and salivary gland toxicity: why does it matter? J Nucl Med 2018.

15. Kabasakal L, AbuQbeitah M, Aygun A, Yeyin N, Ocak M, Demirci E, *et al.* Pre-therapeutic dosimetry of normal organs and tissues of (177)Lu-PSMA-617 prostate-specific membrane antigen (PSMA) inhibitor in patients with castration-resistant prostate cancer. Eur J Nucl Med Mol Imaging 2015;42(13):1976-83.

16. Kratochwil C, Giesel FL, Leotta K, Eder M, Hoppe-Tich T, Youssoufian H, *et al.* PMPA for nephroprotection in PSMA-targeted radionuclide therapy of prostate cancer. J Nucl Med 2015;56(2):293-8.

17. Zechmann CM, Afshar-Oromieh A, Armor T, Stubbs JB, Mier W, Hadaschik B, *et al.* Radiation dosimetry and first therapy results with a (124)I/ (131)I-labeled small molecule (MIP-1095) targeting PSMA for prostate cancer therapy. Eur J Nucl Med Mol Imaging 2014;41(7):1280-92.

18. Kratochwil C, Bruchertseifer F, Rathke H, Bronzel M, Apostolidis C, Weichert W, *et al.* Targeted Alpha Therapy of mCRPC with 225Actinium-PSMA-617: Dosimetry estimate and empirical dose finding. J Nucl Med 2017.

19. Chatalic KL, Heskamp S, Konijnenberg M, Molkenboer-Kuenen JD, Franssen GM, Clahsen-van Groningen MC, *et al.* Towards Personalized Treatment of Prostate Cancer: PSMA I&T, a Promising Prostate-Specific Membrane Antigen-Targeted Theranostic Agent. Theranostics 2016;6(6):849-61.

20. Maurer T, Eiber M, Schwaiger M, Gschwend JE. Current use of PSMA-PET in prostate cancer management. Nat Rev Urol 2016;13(4):226-35.

21. Delker A, Fendler WP, Kratochwil C, Brunegraf A, Gosewisch A, Gildehaus FJ, *et al.* Dosimetry for (177)Lu-DKFZ-PSMA-617: a new radiopharmaceutical for the treatment of metastatic prostate cancer. Eur J Nucl Med Mol Imaging 2016;43(1):42-51.

22. Baum RP, Kulkarni HR, Schuchardt C, Singh A, Wirtz M, Wiessalla S, *et al.* 177Lu-Labeled Prostate-Specific Membrane Antigen Radioligand Therapy of Metastatic Castration-Resistant Prostate Cancer: Safety and Efficacy. J Nucl Med 2016;57(7):1006-13.

23. Roll W, Brauer A, Weckesser M, Bogemann M, Rahbar K. Long-term Survival and Excellent Response to Repeated 177Lu-Prostate-Specific Membrane Antigen 617 Radioligand Therapy in a Patient With Advanced Metastatic Castration-Resistant Prostate Cancer. Clin Nucl Med 2018.

24. Kulkarni H, Schuchardt C, SINGH A, Langbein T, Baum R. Early initiation of Lu-177 PSMA radioligand therapy prolongs overall survival in metastatic prostate cancer. Journal of Nuclear Medicine 2018;59(supplement 1):529.

25. Majer P, Jancarik A, Krecmerova M, Tichy T, Tenora L, Wozniak K, *et al.* Discovery of Orally Available Prodrugs of the Glutamate Carboxypeptidase II (GCPII) Inhibitor 2-Phosphonomethylpentanedioic Acid (2-PMPA). J Med Chem 2016;59(6):2810-9.

26. Chen Y, Pullambhatla M, Foss CA, Byun Y, Nimmagadda S, Senthamizhchelvan S, *et al.* 2-(3-{1-Carboxy-5-[(6-[18F]fluoro-pyridine-3-carbonyl)-amino]-pentyl}-ureido)-pen tanedioic acid, [18F]DCFPyL, a PSMA-based PET imaging agent for prostate cancer. Clin Cancer Res 2011;17(24):7645-53.

27. Rowe SP, Macura KJ, Mena E, Blackford AL, Nadal R, Antonarakis ES, *et al.* PSMA-Based [(18)F]DCFPyL PET/CT Is Superior to Conventional Imaging for Lesion Detection in Patients with Metastatic Prostate Cancer. Mol Imaging Biol 2016;18(3):411-9.

28. Thorek DL, Watson PA, Lee SG, Ku AT, Bournazos S, Braun K, *et al.* Internalization of secreted antigen-targeted antibodies by the neonatal Fc receptor for precision imaging of the androgen receptor axis. Sci Transl Med 2016;8(367):367ra167.

29. Nedelcovych M, Dash RP, Tenora L, Zimmermann SC, Gadiano AJ, Garrett C, *et al.* Enhanced Brain Delivery of 2-(Phosphonomethyl)pentanedioic Acid Following Intranasal Administration of Its gamma-Substituted Ester Prodrugs. Mol Pharm 2017;14(10):3248-57.

30. Fendler WP, Reinhardt S, Ilhan H, Delker A, Boning G, Gildehaus FJ, *et al.* Preliminary experience with dosimetry, response and patient reported outcome after 177Lu-PSMA-617 therapy for metastatic castration-resistant prostate cancer. Oncotarget 2017;8(2):3581-90.

31. Hohberg M, Eschner W, Schmidt M, Dietlein M, Kobe C, Fischer T, *et al.* Lacrimal Glands May Represent Organs at Risk for Radionuclide Therapy of Prostate Cancer with [(177)Lu]DKFZ-PSMA-617. Mol Imaging Biol 2016;18(3):437-45.

32. Kabasakal L, Toklu T, Yeyin N, Demirci E, Abuqbeitah M, Ocak M, *et al.* Lu-177-PSMA-617 Prostate-Specific Membrane Antigen Inhibitor Therapy in Patients with Castration-Resistant Prostate Cancer: Stability, Bio-distribution and Dosimetry. Mol Imaging Radionucl Ther 2017;26(2):62-8.

33. Scarpa L, Buxbaum S, Kendler D, Fink K, Bektic J, Gruber L, *et al.* The (68)Ga/(177)Lu theragnostic concept in PSMA targeting of castration-resistant prostate cancer: correlation of SUVmax values and absorbed dose estimates. Eur J Nucl Med Mol Imaging 2017;44(5):788-800.

34. Yadav MP, Ballal S, Tripathi M, Damle NA, Sahoo RK, Seth A, *et al.* Post-therapeutic dosimetry of 177Lu-DKFZ-PSMA-617 in the treatment of patients with metastatic castration-resistant prostate cancer. Nucl Med Commun 2017;38(1):91-8.

35. Bodei L, Cremonesi M, Ferrari M, Pacifici M, Grana CM, Bartolomei M, *et al.* Long-term evaluation of renal toxicity after peptide receptor radionuclide therapy with 90Y-DOTATOC and 177Lu-DOTATATE: the role of associated risk factors. Eur J Nucl Med Mol Imaging 2008;35(10):1847-56.

36. Kopka K, Benesova M, Barinka C, Haberkorn U, Babich J. Glu-Ureido-Based Inhibitors of Prostate-Specific Membrane Antigen: Lessons Learned During the Development of a Novel Class of Low-Molecular-Weight Theranostic Radiotracers. J Nucl Med 2017;58(Suppl 2):17s-26s.

37. Benesova M, Umbricht CA, Schibli R, Muller C. Albumin-Binding PSMA Ligands: Optimization of the Tissue Distribution Profile. Mol Pharm 2018;15(3):934-46.

38. Zang J, Fan X, Wang H, Liu Q, Wang J, Li H, *et al.* First-in-human study of (177)Lu-EB-PSMA-617 in patients with metastatic castration-resistant prostate cancer. Eur J Nucl Med Mol Imaging 2018.

39. Schmidt A, Wirtz M, Farber SF, Osl T, Beck R, Schottelius M, *et al.* Effect of Carbohydration on the Theranostic Tracer PSMA I&T. ACS Omega 2018;3(7):8278-87.

40. Choy CJ, Ling X, Geruntho JJ, Beyer SK, Latoche JD, Langton-Webster B, *et al.* (177)Lu-Labeled Phosphoramidate-Based PSMA Inhibitors: The Effect of an Albumin Binder on Biodistribution and Therapeutic Efficacy in Prostate Tumor-Bearing Mice. Theranostics 2017;7(7):1928-39.

41. Matteucci F, Mezzenga E, Caroli P, Di Iorio V, Sarnelli A, Celli M, *et al.* Reduction of (68)Ga-PSMA renal uptake with mannitol infusion: preliminary results. Eur J Nucl Med Mol Imaging 2017;44(13):2189-94.

42. van Kalmthout LWM, Lam M, de Keizer B, Krijger GC, Ververs TFT, de Roos R, *et al.* Impact of external cooling with icepacks on (68)Ga-PSMA uptake in salivary glands. EJNMMI Res 2018;8(1):56.

43. Baum RP, Langbein T, Singh A, Shahinfar M, Schuchardt C, Volk GF, *et al.* Injection of Botulinum Toxin for Preventing Salivary Gland Toxicity after PSMA Radioligand Therapy: an Empirical Proof of a Promising Concept. Nucl Med Mol Imaging 2018;52(1):80-1.

44. Valkema R, Pauwels SA, Kvols LK, Kwekkeboom DJ, Jamar F, de Jong M, *et al.* Long-term follow-up of renal function after peptide receptor radiation therapy with (90)Y-DOTA(0),Tyr(3)-octreotide and (177)Lu-DOTA(0), Tyr(3)-octreotate. J Nucl Med 2005;46 Suppl 1:83s-91s.

45. Murga JD, Moorji SM, Han AQ, Magargal WW, DiPippo VA, Olson WC. Synergistic co-targeting of prostate-specific membrane antigen and androgen receptor in prostate cancer. Prostate 2015;75(3):242-54.

46. Antonarakis ES, Lu C, Wang H, Luber B, Nakazawa M, Roeser JC, *et al.* AR-V7 and resistance to enzalutamide and abiraterone in prostate cancer. N Engl J Med 2014;371(11):1028-38.

47. Haberkorn U, Giesel F, Morgenstern A, Kratochwil C. The Future of Radioligand Therapy: alpha, beta, or Both? J Nucl Med 2017;58(7):1017-8.

48. Kratochwil C, Bruchertseifer F, Rathke H, Bronzel M, Apostolidis C, Weichert W, *et al.* Targeted alpha-Therapy of Metastatic Castration-Resistant Prostate Cancer with (225)Ac-PSMA-617: Dosimetry Estimate and Empiric Dose Finding. J Nucl Med 2017;58(10):1624-31.

49. Kratochwil C, Bruchertseifer F, Rathke H, Hohenfellner M, Giesel FL, Haberkorn U, *et al.* Targeted Alpha Therapy of mCRPC with (225)Actinium-PSMA-617: Swimmer-Plot analysis suggests efficacy regarding duration of tumor-control. J Nucl Med 2018.

50. Gaertner FC, Halabi K, Ahmadzadehfar H, Kurpig S, Eppard E, Kotsikopoulos C, *et al.* Uptake of PSMA-ligands in normal tissues is dependent on tumor load in patients with prostate cancer. Oncotarget 2017;8(33):55094-103.

FIGURE LEGENDS

Figure 1. JHU-2545 preferentially delivers 2-PMPA to mouse salivary glands and kidneys versus prostate cancer xenografts. Mice bearing subcutaneous C4-2 prostate cancer xenografts were administered JHU-2545 (3 mg/kg molar equivalent to 2-PMPA, i.v.). 2-PMPA concentrations were monitored over time in plasma, kidneys, salivary glands, and tumor xenograft by LC-MS. JHU-2545 administration resulted in significantly higher 2-PMPA exposures in the kidneys and salivary glands compared to tumor. Data represented as mean or mean ± SEM.

Figure 2. JHU-2545 pre-treatment dose-dependently attenuated uptake of ^{68}Ga-PSMA-11 in rat kidneys. JHU-2545 (1 or 10mg/kg, i.v.) or saline was administered to rats 30 minutes prior to ^{68}Ga-PSMA-11 (42±5 MBq) bolus dosing. A) PET images showed greater cortical renal uptake in control animals (top) compared to animals treated with JHU-2545 (bottom). JHU-2545 treated rats show rapid renal flux with activity passing into the bladder. B) Time activity curves (TAC) show a dose-dependent effect. C) Quantification using the trapezoid method shows a significant, dose-dependent reduction in ^{68}Ga-PSMA-11 area under the curve (AUC). Data represented as mean ± SEM; *p<0.05, **p<0.01.

Figure 3. JHU-2545 pre-treatment attenuated uptake of ^{18}F-DCFPyL in mouse salivary glands and kidneys but not prostate cancer xenografts. A) JHU-2545 (5mg/kg, i.v.) or vehicle was administered to mice 5, 15, or 60 minutes prior to ^{18}F-DCFPyL (7.4-9MBq) bolus dosing. Time activity curves showed that 15-minute pre-treatment provides maximal shielding of kidneys and salivary glands. B) JHU-2545 (0.05-5mg/kg, i.v.) was administered 15 minutes prior to ^{18}F-DCFPyL bolus dosing. Dose-dependent shielding of kidneys and salivary glands was observed with peak effect between 0.2 and 1mg/kg. C) Representative PET images of kidneys and salivary glands at the indicated JHU-2545 dose. D) JHU-2545 (0.25 mg/kg, i.v.) or vehicle was administered to mice bearing subcutaneous 22RV1 prostate cancer xenografts 15 minutes prior to ^{18}F-DCFPyL bolus dosing. JHU-2545 treatment significantly reduced kidney and salivary gland uptake of ^{18}F-DCFPyL at 1 hour post-tracer administration with no effect on tumor xenograft uptake, resulting in increased tumor:kidney and tumor:salivary uptake ratios. Data represented as mean or mean ± SEM; ***p<0.001.

Figure 4. JHU-2545 pre-treatment attenuated uptake of ^{68}Ga-PSMA-617 in mCRPC patient salivary glands and kidneys but not metastases. Representative PET images of mCRPC patient 1 hour after administration of ^{68}Ga-PSMA-617 (235 MBq, 20 nmol, i.v.) without (left) or with (right) JHU-2545 (10mg, i.v.) pre-treatment. SUV_{max} values quantified in table.

Figure 5. JHU-2545 pre-treatment attenuated ^{177}Lu-PSMA-617 doses in mCRPC patient salivary glands and kidneys but not metastases. A) Diagnostic PET scan with ^{68}Ga-PSMA-617 (left) and subsequent time-dependent planar imaging after administration of ^{177}Lu-PSMA-617 (7.4 GBq, 150 nmol, i.v.) with JHU-2545 (10mg) 15-minute pre-treatment (right) in a representative mCRPC patient. B) Quantification of total radiation dose (Gy/GBq) absorbed by kidneys, salivary

glands, and metastases in historical controls (black fill) versus JHU-2545 pre-treated mCRPC patients (red fill). Data represented as mean ± SD.

Figure 1

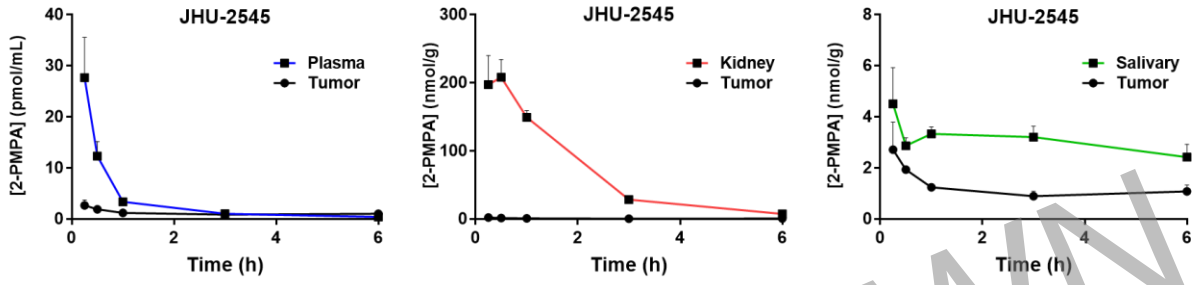

JHU-2545 Pharmacokinetic Parameters

Tissue	C_{max} (nmol/mL or nmol/g)	AUC_{0-t} (h*nmol/mL or h*nmol/g)	Tissue:Tumor AUC Ratio
Plasma	2.72 ± 0.62	6.79 ± 0.19	1.00
Tumor	27.7 ± 4.55	17.8 ± 1.02	2.62
Salivary	4.63 ± 0.73	18.0 ± 0.97	2.65
Kidney	226 ± 8.26	359 ± 4.16	52.9

Figure 2

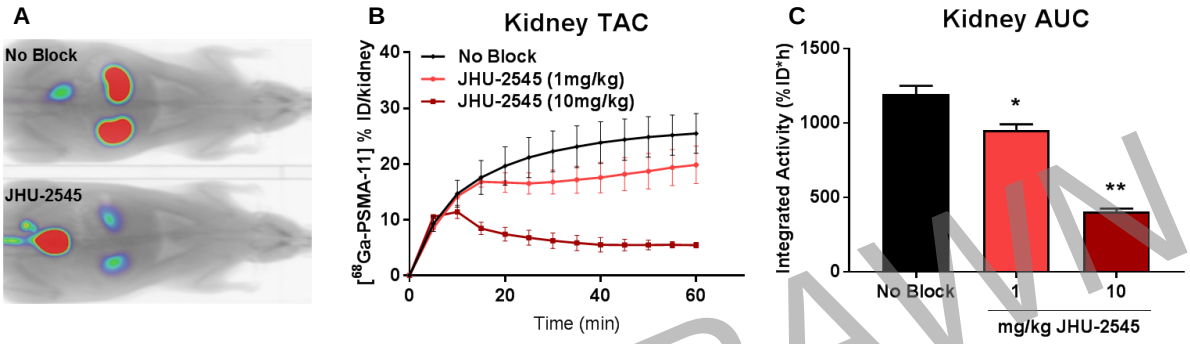

Figure 3

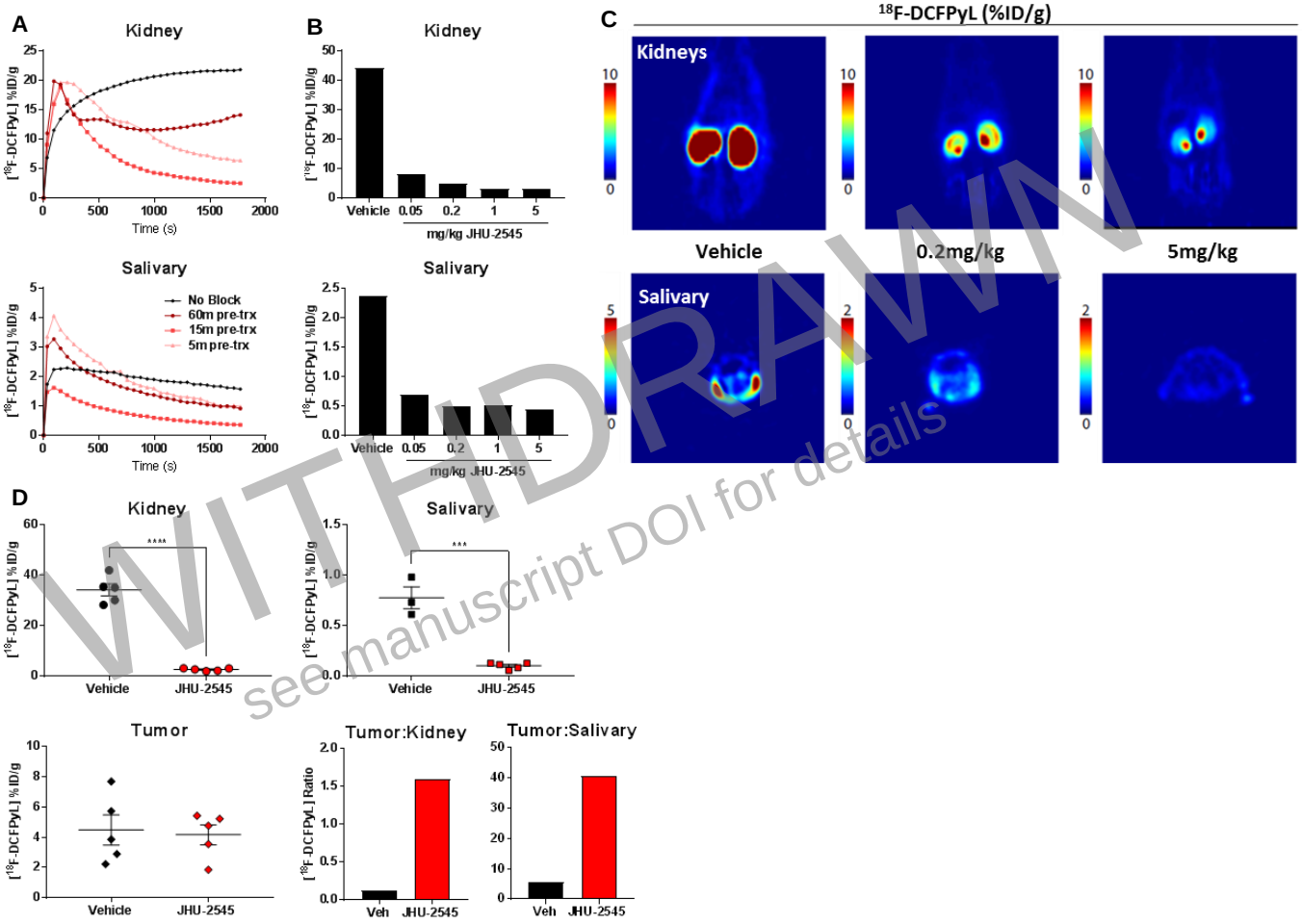

Figure 4

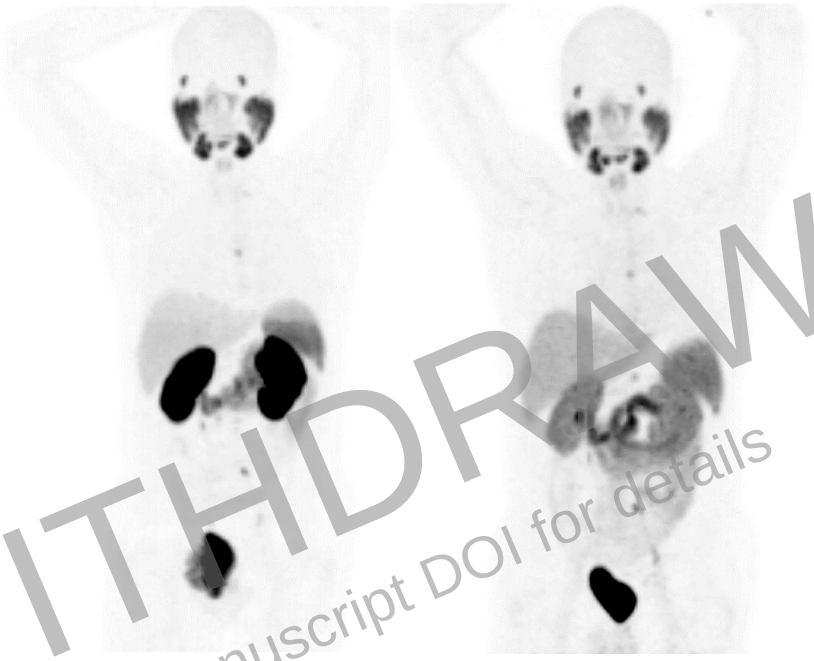

Control ^{68}Ga-PSMA-617 **JHU-2545 + ^{68}Ga-PSMA-617**

Tissue/Organ	Control (SUV_{max})	JHU-2545 (SUV_{max})	% Change
Metastases (mean)	-	-	-3.2
Cervical LN	3.6	3.9	8.3
Thoracic LN	7.8	5.3	-32.1
Parailliacal LN	12.5	8.8	-29.6
Retrocrural LN	4.4	4.2	-4.5
Left Illiacal LN	3.8	5.4	42.1
Salivary (mean)	-	-	-36.7
Parotid	18.2	10.6	-41.8
Submandibular	23.1	14.6	-36.8
Sublingual	13.7	9.4	-31.4
Kidneys	35.4	8.5	-76.0
Lacrimal	16.1	8.9	-44.7
Red Marrow	1.2	1.7	41.7

Figure 5

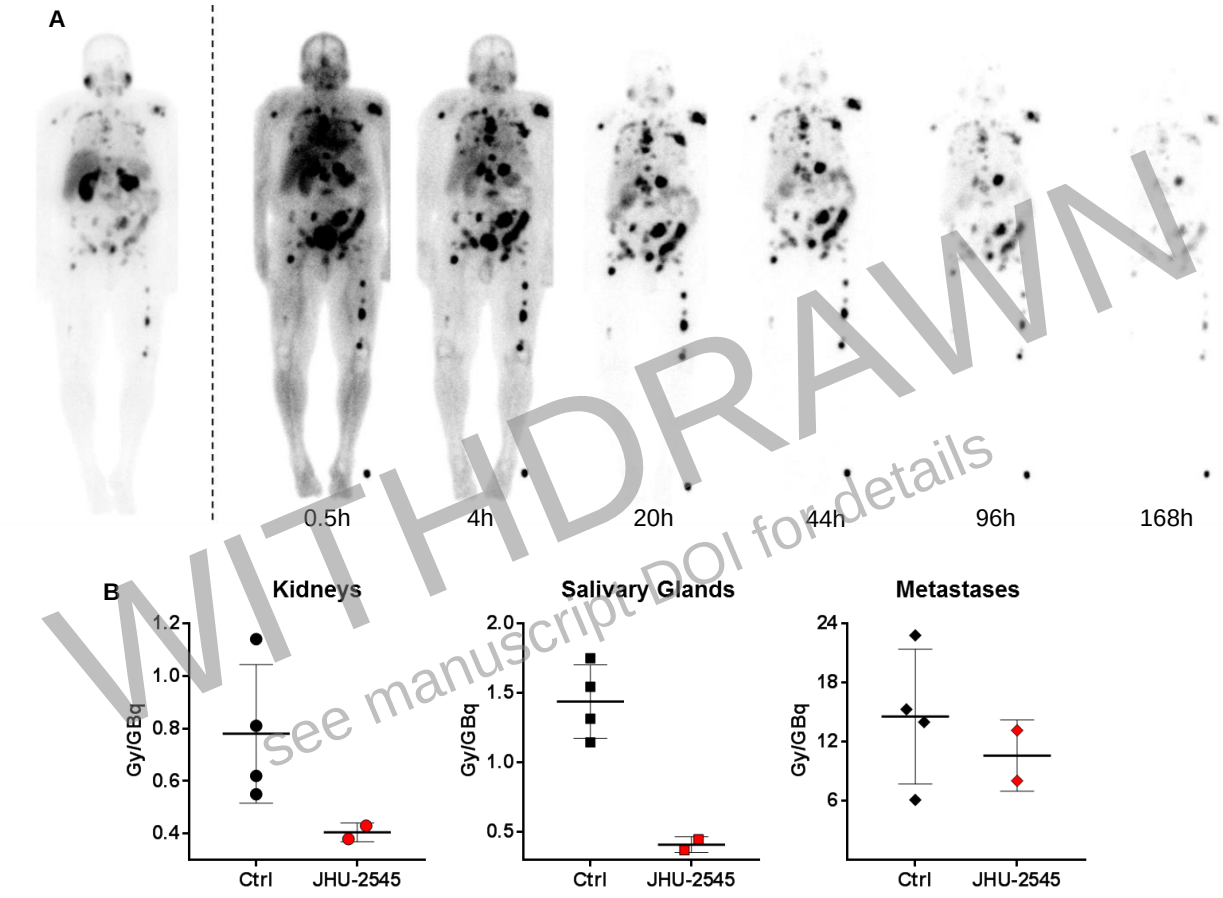

Table 1. ^{177}Lu-PSMA-617 metastases:organ dose ratios for JHU-2545 pre-treated vs. control mCRPC patients

	JHU-2545		Control	
Tissue	Patient 1	Patient 2	Fendler, 2017	Scarpa, 2017
Metastases (mean)	1.0	1.0	1.0	1.0
Salivary (mean)	21.7	29.2	6.1	5.3
Kidneys	21.1	30.6	11.1	4.7
Lacrimal	18.7	16.0	-	2.8
Red marrow	161	329	3,050	70.0